

Plasma spectroscopy of electric spark discharge between silver granules immersed in water

Volodymyr Ninyovskij,

Aleksandr Murmantsev,

Anatoly Veklich,

Vyacheslav Boretskij

*Taras Shevchenko National University
of Kyiv,
Volodymyrska St. 64/13,
01601 Kyiv, Ukraine
Email: ninjovskyj0volodymyr@gmail.com*

This work is devoted to optical emission spectroscopy of plasma of underwater electric discharge, which is used for the synthesis of silver nanoparticles. The main aim of this work is to investigate the possibility and validity of using plasma optical emission spectroscopy to determine its main physical characteristics, such as excitation temperature, electron density, the degree of ionization, etc.

The specially developed pulse power source was used to initiate a discharge between silver granules immersed into the deionized water. Typical values of voltage vary from 40 to 200 V, the current is up to 150 A, and pulse frequency is in the range of 0.2–2 kHz. Applied to electrodes, the voltage caused a current flow along the chain of closely arranged granules in the stochastic switching mode.

Special attention is paid to methods of spectrum treatment of underwater discharge plasma between silver granules. The method of Boltzmann plots and the method of relative intensities on the basis of both atomic and ionic silver spectral lines are used in order to determine the excitation temperature. The spectral lines, which were investigated and treated in detail, were used.

Exposed to the Stark mechanism of spectral line broadening, the spectral profile of H α spectral line is used to determine the electron density. The degree of ionization of the studied plasma was calculated using the obtained values of the electron density and temperature.

Keywords: emission, plasma parameters, underwater discharge, silver granules, Stark effect

INTRODUCTION

Today, interest in the underwater discharge applications (particularly plasma of such discharges) is increasing. On the one hand, it is due to the need to clarify the physical processes of current flow in such environment, and on the other hand, due to its practical application in biology, chemistry and electrochemistry. A special place in the variety of its applications is, in fact, the generation of nanoparticles of conducting materials [1].

For example, magnetic iron oxide nanoparticles are becoming widely used in biomedical applications for developing magnetic resonance imaging contrast agents as well as biocompatible and biodegradable drug carriers [2]. In turn, cobalt and nickel nanomaterials with their oxides are the potential for use in catalytic systems, magnetic materials, semi-conductor and bio-sensors [3]. Moreover, the colloidal solutions with nanoparticles of different metals (in particular, copper, silver, molybdenum, etc.) have excellent bactericidal,

antiviral, antifungal, and antiseptic effects [4], which makes them essential biocide products. The use of direct radiation of plasma of underwater discharge makes it possible to increase the rate of growth and evolution of plants for agricultural needs [5].

In particular, in the past few decades silver nanoparticles have been gaining much attention and have been used in almost every field, including medicine, catalysis, biosensing, drug delivery, electronics, textile, photonics, optical sensor, nonlinear optical properties, water treatment, pigments, photographic, bactericide, anticancer agent, wound treatment, conductive composites, etc. [6].

The materials made of silver are of great practical interest due to the peculiarities and variety of its utilisation. Silver nanoparticles have antiseptic properties and can be effectively used in the different fields of technology, cosmetic industry, household chemicals, food industry, medicine, and in pharma industry, in particular for the production of hydrogels, films for burn and wound treatment, composition implants, ointments, sprays, infiltration of napkins [7] etc. Non-toxicity, sedimentation, and chemical resistances are the most important requirements for such nanoparticles.

Direct investigation of the process, which occurs during nanoparticle formation in order to

improve the characteristics and properties of solutions with nanoparticles, is necessary. In particular, the plasma of discharges, which initiates between granules used as a source of metal particles in the obtained solutions, should be studied. The most suitable approach to such investigation is optical emission spectroscopy. On the one hand, this method enables obtaining the main plasma parameters with sufficient accuracy, such as temperature and electron density, which characterise the processes of nanoparticles formation. On the other hand, such a technique does not perturb the plasma and cannot affect the properties of the resulting product [8].

Considering all the above, the main aim of this work was to investigate the possibilities of using optical emission spectroscopy techniques for the diagnostic of underwater discharge plasma between different metal granules, specifically silver, as well as to determine the key plasma parameters of such discharge, namely, excitation temperature and electron density.

EXPERIMENTAL SETUP

The synthesis of metal nanoparticles in liquid is provided by a specially developed setup (Fig. 1).

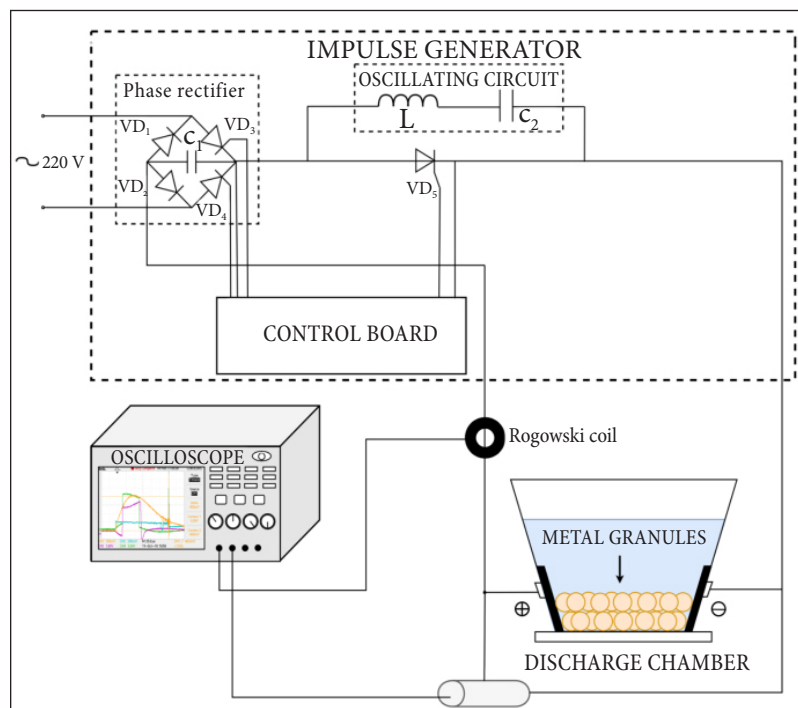


Fig. 1. Experimental arrangement for pulsed underwater electrical discharge investigation [1]

Metal granules of cylindrical form about 1 mm in diameter were placed in a discharge chamber, filled with deionized water. The impulse generator, powered from the single-phase 220 V alternating current network of 50 Hz frequency, was connected with a chamber by electrodes installed into its walls. A composition of power diodes (VD_1 and VD_2) and thyristors (VD_3 and VD_4) rectifies and filters an input voltage. The input energy accumulated into working capacitor C_1 with variable capacity (discretely from 25 to 650 μF), which made it possible to control the power supplied to the granules.

The spark microdischarges between random pairs of metal granules were initiated due to rapid switching of the thyristor VD_5 . Control of the switching moment of this thyristor was provided by a half-period of free oscillations of the LC_2 oscillatory contour. Finally, the control board made it possible to regulate the voltage, frequency, and the duty cycle of impulses through power thyristors.

The discharges that occurred in stochastic switching mode in the chamber led to the destruction of some metal granules, which, in turn, led to the creation of a vapour phase of conductive material near the surface of the granules. After contact with water, these vapours were rapidly cooled, which led to the formation of nanoparticles. This process of discharge burning was accompanied by the creation of plasma, which could be ob-

served via a quartz window installed into the wall of the discharge chamber. The Solar LS SDH-IV spectrometer was oriented in front of this window, which allowed registering the emission spectra in the range from 440 to 910 nm. Calibration of spectral sensitivity (see Fig. 2) of such a device was carried out by a tungsten ribbon lamp.

The excitation temperature, obtained by Boltzmann plots technique based on emission intensities and spectroscopic data of the used atomic silver spectral lines, can be determined as follows:

$$-\frac{E_k}{kT} = \ln \left[\frac{I\lambda^3}{g_i f_{ik}} \right] + C, \quad (1)$$

where E_k is the energy of the upper level of spectral transition, k is the Boltzmann constant, T is the excitation temperature, I is the intensity of spectral line emission, λ is the wavelength of a spectral line, g_i is the statistic weight for the lower energy level, f_{ik} is the oscillation strength of the corresponding transition, $C = \ln \left[\frac{m\Sigma}{2\pi n h l e^2} \right]$, m is the electron mass, Σ is the partition function of the atom, n is the concentration of atoms on the ground energy level, h is the Planck constant, l is the length of radiating layer, e is the electron charge.

Additionally, the excitation temperature was determined by the method of relative intensities of ionic spectral lines according to the equation:

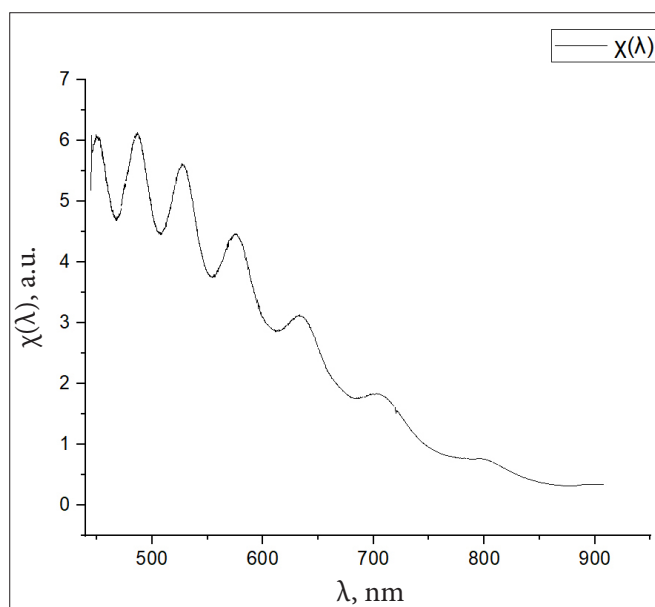


Fig. 2. Spectral sensitivity of the spectrometer $\chi(\lambda)$ [9]

$$T[K] = \frac{E_2 - E_1}{k \ln \left[\frac{I_1 A_2 g_2 \lambda_1}{I_2 A_1 g_1 \lambda_2} \right]}, \quad (2)$$

where $E_{1,2}$ are energies of the upper levels of ionic spectral lines, k is the Boltzmann constant, T is the excitation temperature, $I_{1,2}$ are intensities of spectral line emission, $\lambda_{1,2}$ are corresponding wavelength, $g_{1,2}$ are statistic weights for the upper energy levels, $A_{1,2}$ are transition probabilities.

The electron density in plasma of underwater discharge between silver granules was determined from the full width at half maximum (FWHM) of the profile of H_α Balmer spectral line. In the case when a linear Stark effect is a dominant broadening mechanism of this line, the electron density can be calculated as follows [10, 11]:

$$n_e [m^{-3}] = 10^{23} \times \left(\frac{w_s [nm]}{1.098} \right)^{1.47135}, \quad (3)$$

where w_s is the Stark width of H_α spectral line, broadened due to Stark effect.

The Voigt function was used for spectral line approximation to determine both the emission

intensity and FWHM. The necessity of utilisation of this approach is caused by the importance of accounting the instrument function of the used spectrometer.

The degree of ionization of plasma of underwater discharge between silver granules can be calculated by the Saha equation:

$$\eta = \frac{n_i}{n_a} = \frac{2}{n_e} \frac{\Sigma_i}{\Sigma_a} \left(\frac{2\pi m k T}{h^2} \right)^{\frac{3}{2}} \frac{e^{-\frac{\epsilon}{kT}}}{}, \quad (4)$$

where k is the Boltzmann's constant, T is the excitation temperature, n_i is the concentration of ions, n_a is the concentration of atoms, n_e is the electron density, m is the electron mass, $\Sigma_{a,i}$ are partition functions of atom and ion, respectively, h is the Plank constant, ϵ is the ionization potential of the silver atom (7.57 eV).

RESULTS AND DISCUSSIONS

As an example, Fig. 3 shows the emission spectrum of underwater discharge plasma between silver granules. The atomic and ionic spectral lines of silver and the H_α line are clearly observed in this spectrum.

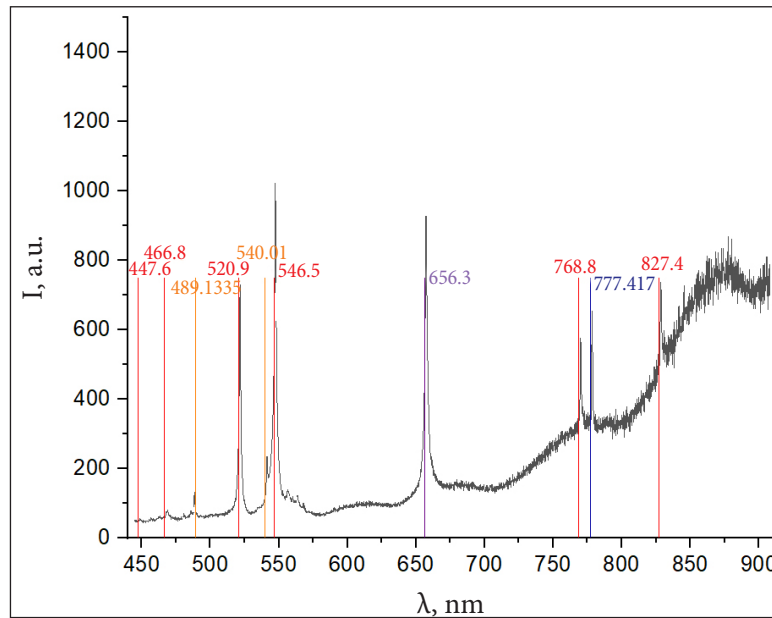


Fig. 3. Emission spectrum of underwater discharge plasma between silver granules. Red curves – silver atomic Ag I; orange curves – silver ionic Ag II; the violet curve – H_α ; the blue curve – O I spectral lines

Moreover, the reference dots, which correspond to the wavelength of the appropriate spectral lines taken from the NIST database [12, 13], are presented in the spectrum. The red lines correspond to the silver atomic spectral lines (Ag I), the orange lines correspond to the ionic lines (Ag II), the violet line is the H_{α} spectral line, and the blue one is the oxygen spectral line. The corresponding spectroscopic data, the determined intensities, and calculated values of $\ln(I\lambda^3/g_i f_{ik})$ for the spectral lines marked in Fig. 3 are presented in Table 1.

Figure 4 shows the diagrams of the energy levels of silver with transition, which correspond to the registered emission spectral lines.

As mentioned above, the electron density is determined from the contour of the hydrogen

H_{α} spectral line. The approximation of this line profile, taking the instrumental function into account, is shown in Fig. 5.

The Gauss component of the Voigt function is used for the deconvolution of the instrumental function of registering spectral device. It was preliminary found that the value of this function was estimated as 0.26 nm. The estimation was carried out using the high-frequency lamp on mercury vapours. With this approach, the Lorentz component of the Voigt function corresponds to Stark width of the spectral line and equals $w_L = w_S = 1.89$ nm. The corresponding electron density is $n_e = 2.2 \cdot 10^{23} \text{ m}^{-3}$.

As mentioned above, the excitation temperature in plasma was determined by the Boltzmann plot technique based on intensities of

Table 1. Spectral lines and spectral data for these lines that were used in this study [12, 13]: λ is the wavelength of the spectral line; g_i, g_k and E_i, E_k are the statistical weights and energies of i and k energy levels, respectively; I is the emission intensity of the spectral line; $\Delta\lambda$ is the FWHM of the spectral line, n_e is the calculated electron density, f_{ik} is the oscillator strength; A_{ki} is the transition probability

λ , nm	$g_i f_{ik}$	E_i , eV	E_k , eV	I , a.u.	$\ln(I\lambda^3/g_i f_{ik})$	$\Delta\lambda$, nm	n_e , m^{-3}	$A_{ki} g_{kr} \text{ s}^{-1}$
Ag I 520.9	1.09	3.66	6.04	1356.49	-36.28	-	-	$3 \cdot 10^8$
Ag I 546.5	2.03	3.78	6.04	2382.12	-36.19	-	-	$5.2 \cdot 10^8$
Ag I 768.8	0.24	3.66	5.28	297.78	-35.11	-	-	-
H_{α} 656.3	5.13	10.2	12.09	-	-	1.89	$2.2 \cdot 10^{23}$	$7.9 \cdot 10^8$
Ag II 489.1	0.00178	11.2	13.74	75.77	-32.93	-	-	$5 \cdot 10^5$
Ag II 540.0	10.47	15.71	18	384.92	-39.69	-	-	$2.3 \cdot 10^9$

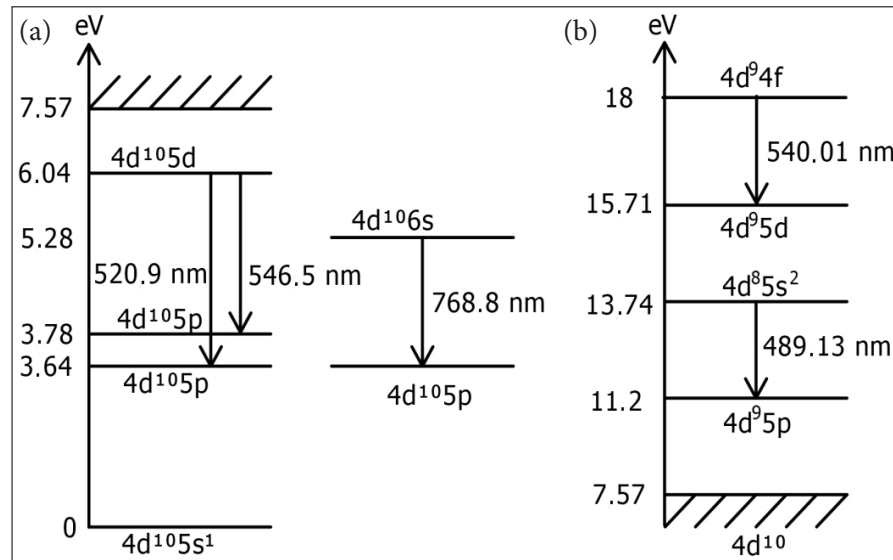


Fig. 4. Simplified diagrams of energy levels of silver with the marked spectral lines, which are used in the diagnostic of underwater discharge plasma between silver granules: (a) atom levels; (b) ion levels

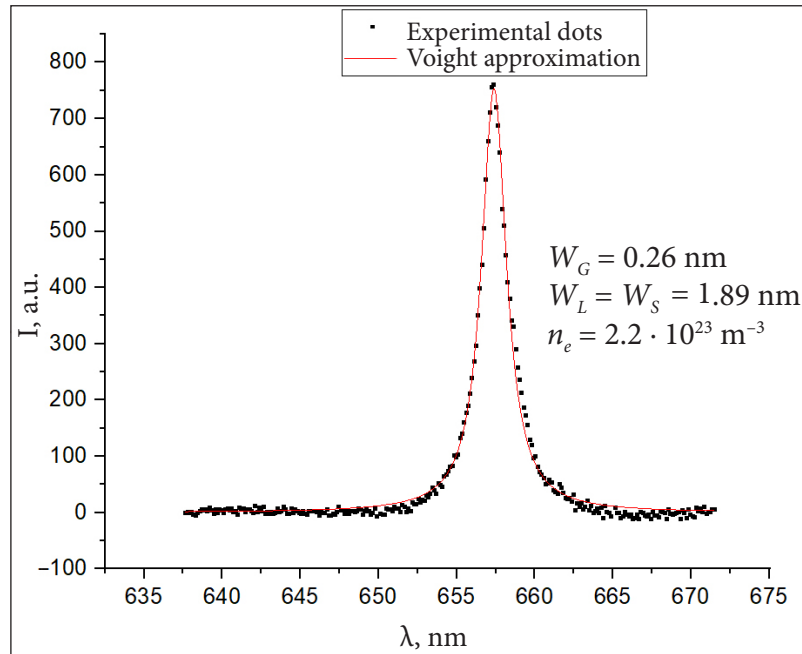


Fig. 5. Approximation by the Voigt function of the H_α spectral line

the emission of atomic silver spectral lines and by the method of the ratio of intensities of ionic spectral lines.

The Boltzmann plot based on atomic silver spectral lines is shown in Fig. 6.

The obtained excitation temperature is $T = 7800 \pm 500$ K. This result is obtained with ex-

perimental error, which was caused by the proximity of values of energies of upper levels of atomic silver spectral lines.

The Boltzmann plot according to the method of relation intensities of Ag II spectral lines is shown in Fig. 7. It should be noted that this method is validated when the difference between

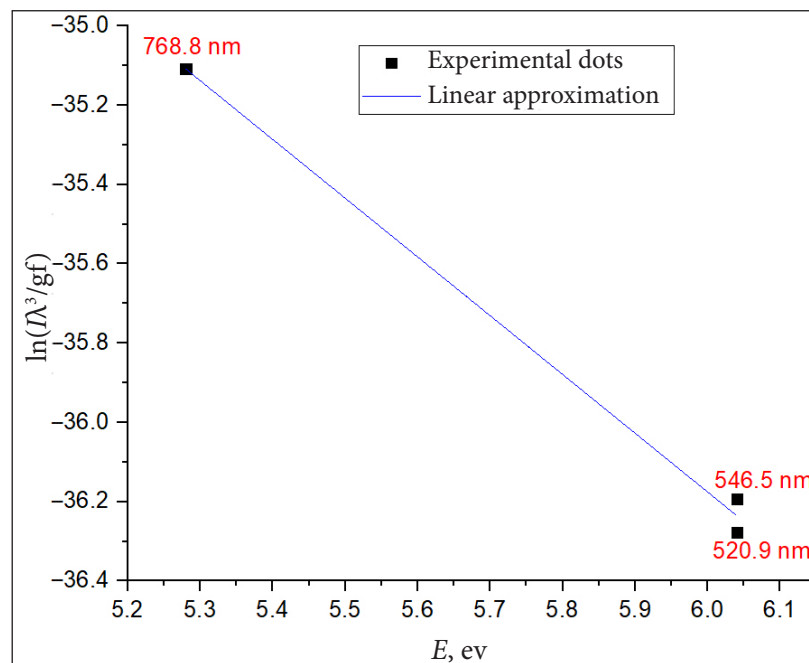


Fig. 6. The Boltzmann plot on the basis of Ag I spectral lines

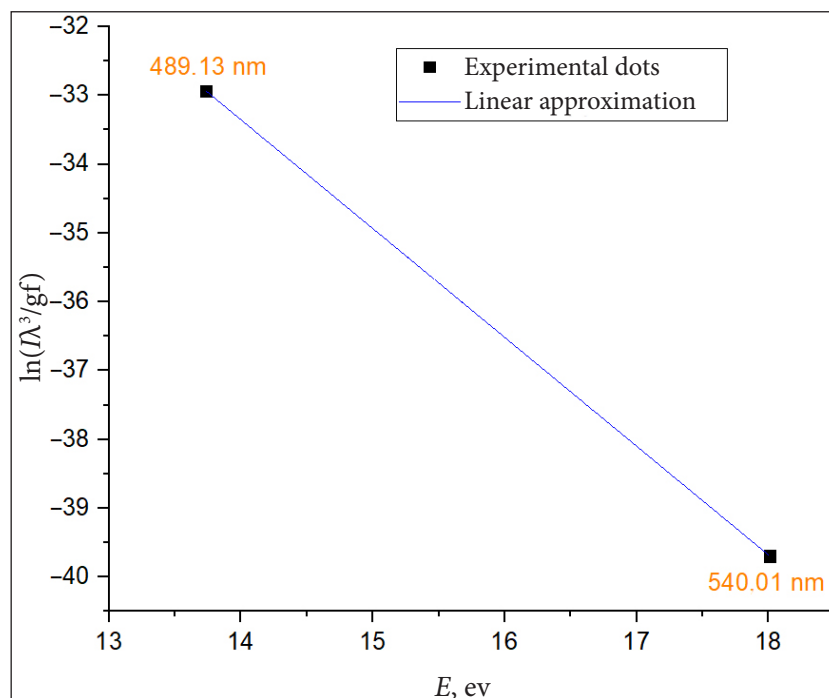


Fig. 7. The Boltzmann plot according to the method of relative intensities of Ag II spectral lines

energies of the upper levels of spectral lines is more than 4 eV. Determined in such a way, the excitation temperature is $T = 7400 \pm 100$ K.

It is evident that excitation temperature, determined both on the basis of atomic and ionic spectral lines, coincides within the frame of the measurement error. Due to this fact, it can be assumed that the investigated plasma may be in the local thermodynamic equilibrium. Therefore this assumption makes it possible to use the Saha equation (4) to estimate the degree of ionization of underwater discharge plasma between silver granules (see Table 2).

Table 2. The degree of ionization of underwater discharge plasma between silver granules

T, K	η
7800	0.098
7400	0.046

One can see that the investigated plasma source fully corresponds to the weakly-ionized plasma model. This fact may be useful in further investigations devoted to estimating the concentration of neutral and charged component of metal in such plasma. Therefore these studies may be

important for optimising the process of generating metal nanoparticles.

CONCLUSIONS

A method for the diagnostics of plasma of underwater discharge between silver granules by optical emission spectroscopy was proposed. Such a plasma source was realised on an original installation, which was specially developed for the synthesis of colloidal substance with metal nanoparticles. Special attention was paid to the methods of spectrum treatment of underwater discharge plasma between silver granules.

For the first time, the electron density in such plasma was determined from the spectral profile of the hydrogen H_{α} Balmer spectral line, which broadened due to the linear Stark effect. The Voigt function was used for approximation of this spectral line, which made it possible to deconvolute the instrumental function of the spectral device. Obtained in this way, the electron density value was $2.2 \cdot 10^{23} \text{ m}^{-3}$.

The method of the Boltzmann plot and the method of relative intensities based on both atomic and ionic silver spectral lines were used to determine the excitation temperature.

It was found that the excitation temperature, obtained by the method of relative intensities of ionic spectral lines ($T = 7400$ K), coincided with the temperature obtained on the basis of atomic spectral lines ($T = 7800$ K), within the frame of the measurement error. This fact makes it possible to assume that the investigated plasma may be in the local thermodynamic equilibrium. In the frame of this assumption, the degree of ionization of such plasma was estimated (did not exceed 0.01).

Received 21 June 2022

Accepted 23 December 2022

References

1. Veklich A., Tmenova T., Zazimko O., Trach V., Lopatko K., Titova L., Boretskij V., Aftandiljants Y., Lopatko S., Rogovskiy I. Regulation of Biological Processes with Complexions of Metals Produced by Underwater Spark Discharge. *Springer Proceedings in Physics*. 2020. Vol. 247. P. 283–306. doi: 10.1007/978-3-030-52268-1_23.
2. Yang L., Cao Z., Sajja H. K., Mao H., Wang L., Geng H., Xu H., Jiang T., Wood W., Nie Sh., Wang Y. A. Development of receptor targeted magnetic iron oxide nanoparticles for efficient drug delivery and tumor imaging. *Journal of Biomedical Nanotechnology*. 2008. Vol. 4. P. 443–449. doi: 10.1166/jbn.2008.007.
3. Merciris T., Valensi F., Hamdan A. Synthesis of nickel and cobalt oxide nanoparticles by pulsed underwater spark discharges. *Journal of Applied Physics*. 2021. Vol. 129. ID 063303. doi: 10.1063/5.0040171.
4. Xiu Z., Zhang Q., Puppala H., Colvin V., Alvarez P., Negligible particle-specific antibacterial activity of silver nanoparticles. *Nano Letters*. 2012. Vol. 12. No. 8. P. 4271–4275. doi: 10.1021/nl301934w.
5. Takaki K., Takahata J., Watanabe S., Satta N., Yamada O., Fujio T., Sasaki Y. Improvements in plant growth rate using underwater discharge. *Journal of Physics: Conference Series*. 2013. Vol. 418. ID. 012140. doi: 10.1088/1742-6596/418/1/012140.
6. Singaravelan R. and Bangaru Sudarsan Alwar S. Electrochemical synthesis, characterisation and phytogenic properties of silver nanoparticles. *Applied Nanosciences*. 2015. Vol. 5. P. 983–991. doi: 10.1007/s13204-014-0396-0.
7. Semenyuk N., Kostiv U., Dsyaman I., Klym Y., Skorohoda V. Osoblyvosti odergannya nano-chastynok sribla u prysutnosti polivinilpirolidonu [Features of obtaining silver nanoparticles in the presence of polyvinyl pyrrolidone]. Lviv: P. 440–441. Ukrainian.
8. Konjevic N., Ivkovic M., Sakan N. Hydrogen Balmer lines for low electron number density plasma diagnostics. *Spectrochimica Acta Part B*. 2012. Vol. 76. P. 16–22. doi: 10.1016/j.sab.2012.06.026
9. Nikiforov A., Leys C., Gonzalez M., Walsh J. Electron density measurement in atmospheric pressure plasma jets: Stark broadening of hydrogenated and non-hydrogenated lines. *Plasma Sources Science Technology*. 2015. Vol. 24. No. 3. ID 034001. doi: 10.1088/0963-0252/24/3/034001.
10. Murmantsev A., Veklich A., Boretskij V. Peculiarities of plasma spectroscopy of underwater electric spark discharge between molybdenum granules. *CYSENI*, 2021. P. 515–524.
11. Venger R., Tmenova T., Valensi F., Veklich A., Cressault Y., Boretskij V. Detailed Investigation of the Electric Discharge Plasma between Copper Electrodes Immersed into Water. *Atoms*. 2017. Vol. 5. ID. 40. doi: 10.3390/atoms5040040.
12. Kramida A., Ralchenko Yu., Reader J. and NIST ASD Team. NIST Atomic Spectra Database (ver. 5.8, 2020). National Institute of Standards and Technology, Gaithersburg, MD. doi: 10.18434/T4W30F
13. Babich I. L., Boretskij V. F., Veklich A. N., Semenyshyn R. V. Spectroscopic data and Stark broadening of Cu I and Ag I spectral lines: Selection and analysis. *Advances in Space Research*. 2014. Vol. 54. Iss. 7. P. 1254–1263. doi: 10.1016/j.asr.2013.10.034

Volodymyr Ninyovskij, Aleksandr Murmantsev, Anatoly Veklich, Vyacheslav Boretskij

VANDENYJE PANARDINTŲ SIDABRO GRANULIŲ ELEKTRINIO KIBIRKŠTINIO IŠLYDŽIO
PLAZMOS SPEKTROKOPIJA